CMS/TN 96-002

Beam Test of a FPGA Prototype of a Front-end Trigger Device for Muon Barrel Chambers

L. Castellani[1], M. Cavicchi[1], M. De Giorgi[1], A. De Min[1], I. Lippi[1], R. Martinelli[1] and P. Zotto[2]

Sezione dell'I.N.F.N. di Padova, Italy

1) Dipartimento di Fisica dell'Università di Padova, Italy
2) Dipartimento di Fisica del Politecnico di Milano, Italy

1. Introduction

The triggering front-end device foreseen in the muon barrel chambers is the Bunch and Track Identifier (BTI), commonly known as *mean-timer*.

The BTI, in its basic version, triggers at the alignment of all the hits in the group of drift tubes interested by the muon. The coincidence of these hits happens at fixed time after the muon traversed the array of drift tubes and the BTI can extract the full track information (slope and intercept). The complete description of the mechanism and the conceptual design of a fully working device is available as CMS/TN 95-01.

Although the device can reasonably be realized only with an ASIC, it can be partially implemented using FPGA technology.

Three prototypes of BTI were produced in 1995 and tested on a muon beam during the summer. The results of the test as well as some simulations of the full scale device, using test data, are summarized in this note.

2. Design of the XILINX Prototype

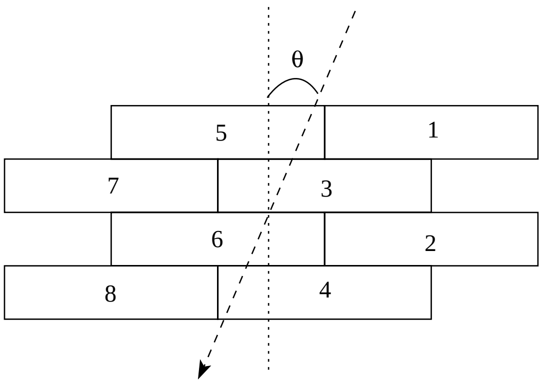

Figure 1 - XILINX prototype BTI allocation in test beam

A prototype realized using FPGA is obviously limited by the available size and speed of the ICs. The implementation of the algorithm encountered serious space limitations, forcing us to downgrade the requirements.

The actual IC used was XILINX XC4013, 6 ns grade.

The BTI prototype was thought as a device programmable for fixed incidence angle, as it is always the case test beam setup. In this case the BTI generates a valid trigger signal when the track is in the programmed range and hence there is no need for an evaluation of the track slope as in the full design. Due to space limitations, no information on position is output from the BTI.

The number of wires, allocated to the prototype as in Figure 1, is 8, instead of 9 as was later foreseen for the complete BTI, and only a subgroup of relevant couples of wires (1-3, 1-6, 2-3, 3-5, 3-6, 3-8, 4-3, 4-5, 4-6, 5-7, 5-8, 6-5, 6-7, 6-8) is considered.

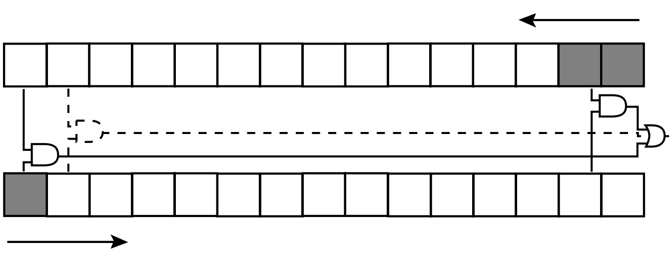

Figure 2 - Shift register of a couple of wires showing acceptance. The input position of the upper shift registers is programmable as a function of the track angle.

As shown in Figure 2, the signals coming from each couple of wires are shifted in opposite directions inside a pair of shift registers whose depth is programmable as a function of the maximum drift-time. The shifting frequency is 40 MHz (compared to 80 MHz of the final VLSI circuit): therefore the shift of one cell corresponds to 25 ns.

At every clock step the AND of the two vertically aligned bits of the shift registers is evaluated. The tolerance allowed in the AND evaluation is built in from the fact that the signal running in the upper shift register is two cells wide, while the signal inside the lower one is only one cell wide. This choice is a compromise between efficiency and noise of the device.

The programmability for fixed angles means that, depending on the chosen angular range and the actual drift velocity, for each wire couple the signals are input to a programmed depth inside the upper shift register and the coincidence is output with a predefined delay, chosen to synchronize each couple. A look-up table, including an initial shift and a delay for each couple, is loaded for each angular configuration.

The couples are grouped in patterns (listed in Table 1), each one including 3 or 4 couples, whose coincidence is evaluated at every clock cycle. Inside each pattern only the couples with the drift in opposite directions are considered. If any two of the couples of the pattern give a coincidence signal a Low Level Trigger (LTRG) is generated, while a High Level Trigger (HTRG) is generated if all the couples of the pattern are available. The information about the triggering pattern and the trigger type is not recorded.

A noise reduction mechanism is available, because the LTRG signal is issued only if at the neighbouring steps there is no HTRG generated.

1-3&2-3&4-3	1-3&1-6&4-3&4-6	1-6&3-6&4-6
3-5&3-6&4-5&4-6	3-6&4-6&6-5	3-5&3-6&3-8
3-5&3-8&6-5&6-8	6-5&6-7&6-8	5-7&5-8&6-7&6-8

Table 1 - List of patterns included in the BTI prototype.

3. Test Setup

A DTBX prototype with four layers of 16 drift tubes each was equipped with three XILINX prototypes staggered by one cell as in the final design. They were tested in the H2 muon beam with a free running clock.

The BTI is a synchronous device and therefore its performance is strictly tied to the synchronization. The recorded TDC data included drift times, BTI generated trigger signals and the BTI clock to allow computing the phase of each event for the BTI with respect to the test beam trigger.

The data were recorded using 2277 Lecroy TDCs, with 1 ns least count and multihit capability, and the XILINX cards were put after 60 m long cables: the difference in delay between signals on different wires caused by the line length was measured with testpulses and was within ±4 ns.

All the data used in the following analysis were taken with tensions V_{anode}=3600 V, V_{anode}=-1800 V and $V_{electrode}$=1800 V and the discriminator threshold was corresponding to 4 pC.

Data were taken at the nominal inclinations of $\theta = 0^0$, $\theta = 10^0$, $\theta = 20^0$ of the beam with respect to the wires and at nominal magnetic field values of B = 0T, B = 0.5T, B = 1T, B=1.5T.

The BTI was programmed for a maximum drift-time T_{MAX} = 350 ns. This programmation was never changed, even when the magnetic field was switched on modifying the actual drift velocity.

Nominal inclination	**$\theta = 0^0$**		**$\theta = 10^0$**		**$\theta = 20^0$**	
Wire Couples	θ min	θ max	θ min	θ max	θ min	θ max
1-3	0	5.9	5.9	12.3	17.8	23.5
1-6	0	3.0	8.8	12.3	17.8	21.0
2-3	0	5.9	5.9	12.3	17.8	23.5
3-5	0	6.5	6.5	12.3	18.4	24.0
3-6	0	5.9	5.9	12.3	17.2	23.5
3-8	0	3.0	9.4	12.3	18.4	21.0
4-3	0	3.0	8.8	12.3	17.8	21.0
4-5	0	2.4	8.3	10.6	18.3	19.9
4-6	0	6.5	6.5	12.3	18.4	23.5
5-7	0	6.5	6.5	12.3	18.4	24.0
5-8	0	2.4	8.3	10.6	18.4	20.4
6-5	0	3.0	9.4	12.3	18.4	21.0
6-7	0	6.5	6.5	12.8	18.4	24.0
6-8	0	6.5	6.5	12.3	18.4	24.0

Table 2 - Acceptance of the programmed wire couples.

The list of implemented couples with the angular ranges of each couple for the nominal inclination programmed is given in Table 2.

4. Results

The major task of the test was the evaluation of the efficiency of the triggering mechanism, being all the other interesting checks ruled out from space limitations in the XILINX implementation of the BTI.

4.1 Efficiency versus Synchronization

The efficiency is defined as the fraction of events giving a BTI trigger at the expected time with respect to the particle crossing (in our setup the 23rd step).

The data were taken asynchronously and therefore the first important check was done on the performance of the BTI as a function of the phase with respect to particle crossing, since we expect that events are assigned the wrong crossing when the phase is lost. The efficiency of the device as a function of the synchronization time is shown in Figure 3 for a sample of data at $\theta = 0^0$ and B = 0T. The efficiency exhibits an almost flat top at ±5 ns from the central value and drops when the BTI clock is too early or too late. A more detailed analysis of the

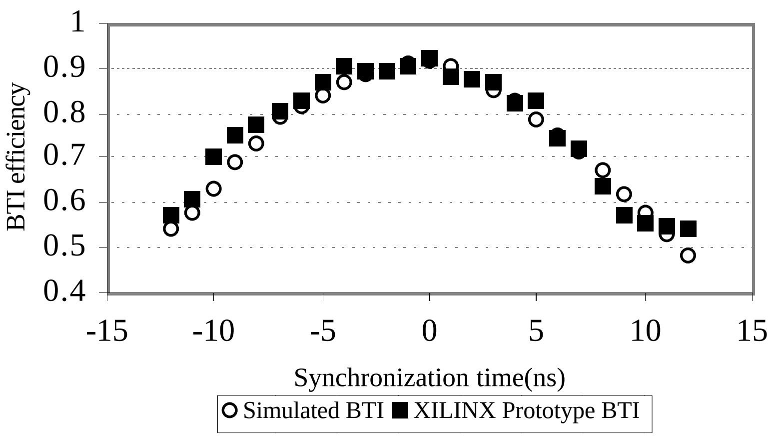

Figure 3 - BTI efficiency vs synchronization with the experiment trigger

data shows that the missing fraction of events is assigned to the step before the expected one if the clock is too early and to the step after the expected one if the clock is too late. The result is confirmed from a simulation of the device using only synchronous data outphased by the wanted time.

4.2 Efficiency versus drift time

The BTI was programmed for a maximum drift-time T_{MAX} = 350 ns, but the actual maximum drift time turned out to be T_{MAX} = 335 ns. The effect on the performance of the bad matching between expected and actual value can be seen in Figure 4, where the efficiency versus the drift time of the wire in the first layer shows a seesaw behaviour with a 25 ns period. This means that close to certain drift-times the device sampling assigns the input signal to the wrong step, and the tight coincidence allowed for the signals is no more verified.

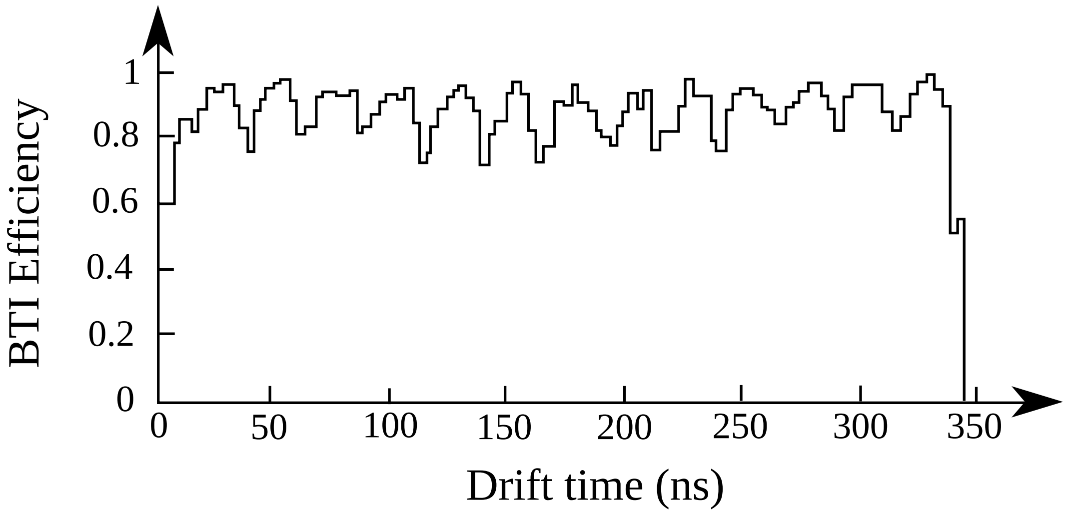

Figure 4 - BTI efficiency as a function of the drift time of the wire in the first layer for θ = 0 sample.

4.3 Comparison of BTIs

The drift times associated to an event can be used to fit a straight line through the four layers. We reconstructed all the tracks with at least 3 points using a fit probability cut at 0.1 % and allowing the rejection of the worst measurement for the 4 points tracks. Then we measured the fraction of events with a reconstructed track in which there was a BTI signal at the expected step.

The request of a fitted track excludes two non negligible contributions to the overall inefficiency. Indeed it factorizes out the contribution of chamber inefficiency, since it excludes from counting the events in which the fit could not be performed due to missing drift times, and the contribution of cases of penetrating δ-rays or electromagnetic showers that spoiled the drift time measurement in more than one cell.

Therefore the quoted efficiency is considering only the effect of soft δ-rays fully contained in a cell.

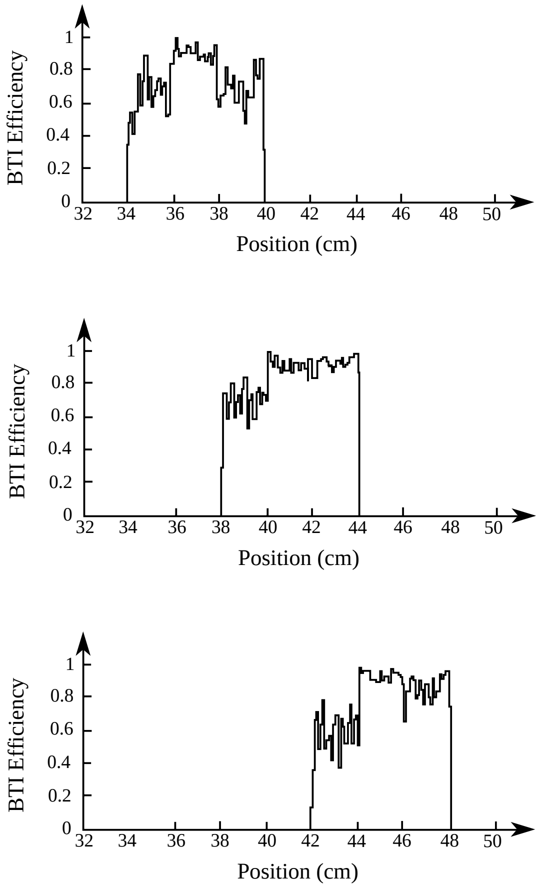

Figure 5 - Efficiency as a function of position for each BTI.

Data were collected using three BTI's. Each of them was covering 6 cm of the chamber, but they were staggered by 4 cm providing a 2 cm superposition between two consecutive devices. The total covered area of the chamber was therefore 14 cm wide.

It is possible to make a comparison of the performance of the three prototypes, looking at the efficiency in the respectively covered areas.

The efficiency of the prototypes is shown as a function of position in Figure 5. It can be immediately noticed that every prototype has a lower efficiency in the first two centimeters covered: this is because the couple 4-2 was on purpose not implemented, because its range is meant to be covered from the previous BTI. On the contrary each BTI was programmed to be fully efficient in the next four centimeters covered.

This is well verified for two of them, while there is an ununderstood inefficiency in the first one. This inefficiency is anyway completely recovered from the superposition of the second one, owing to the existing redundancy, as we can see from Figure 6, where all the BTIs are plotted together.

4.4 Efficiency versus Angle

The track fitting can also be used to investigate the efficiency of the BTI as a function of the angle. The fitted angle for the runs taken without magnetic field is

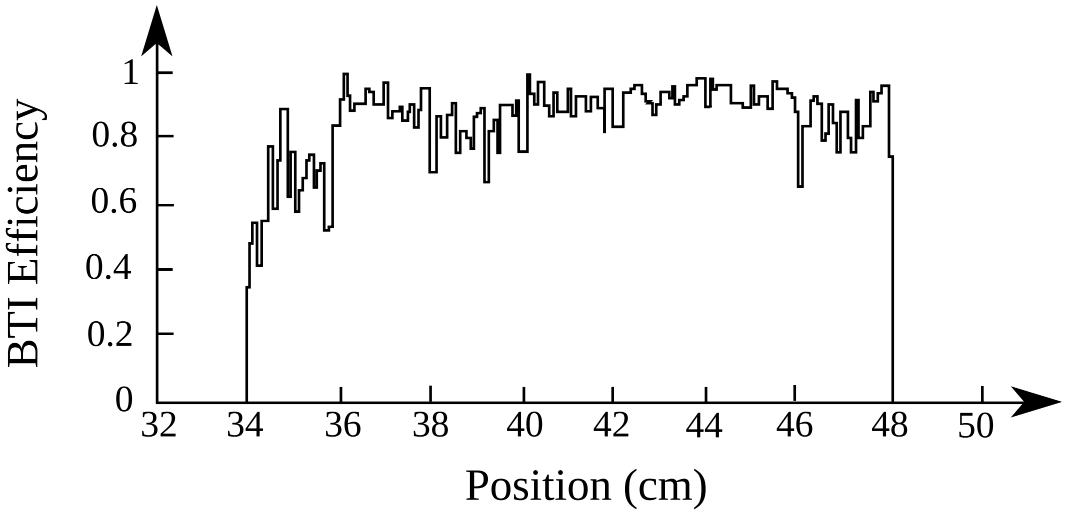

Figure 6 - BTI efficiency as a function of the position in the chamber frame

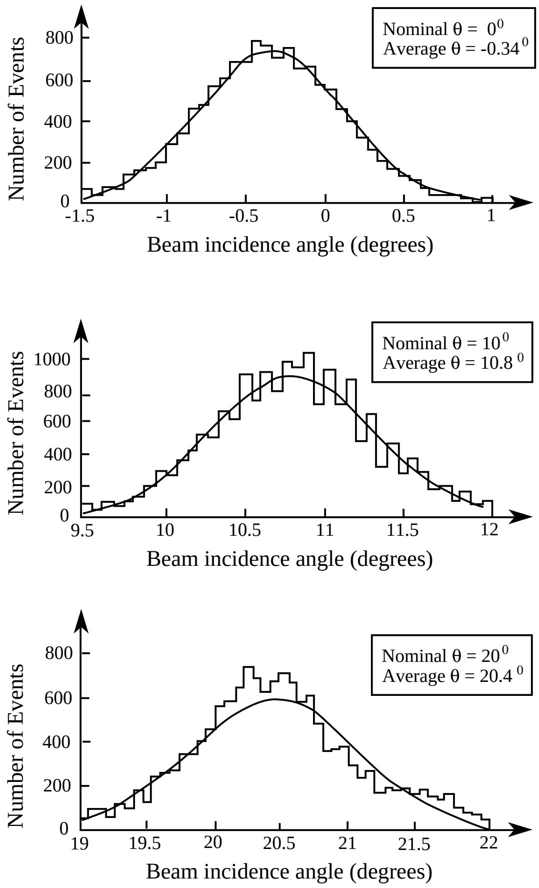

Figure 7 - Fitted beam incidence angle.

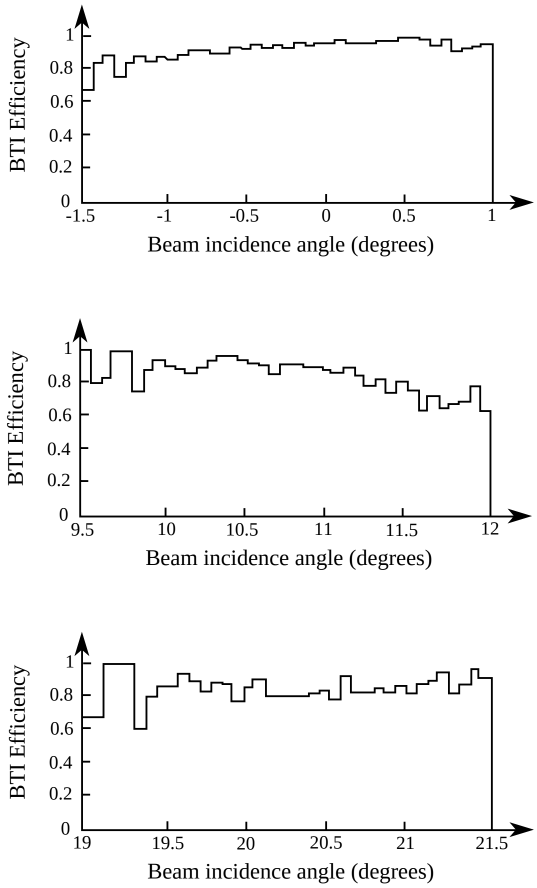

Figure 8 - BTI efficiency as a function of fitted angle.

shown in Figure 7. A glance to Table 1 immediately shows that the angular acceptance of each couple is quite different and that the actual beam incidence angle was rather critical for the performance of the device. In fact the angle for the nominal $\theta = 0^0$ sample was slightly negative, while for the nominal $\theta = 10^0$ and $\theta = 20^0$ samples it was set in a transition region where some couples were fully efficient and others inefficient. Another problem was that in the case of the inclined tracks the portion of chamber equipped with BTIs was off-centred with respect to the beam: in fact only the first BTI was inside the beam spot.

The effect of the uneven angular acceptance of the couples is clearly visible in Figure 8, where the BTI efficiency is plotted as a function of the fitted angle for the three samples of data: the efficiency monotonically decreases as the angle becomes more negative and an efficiency reduction is clearly visible at angles greater than 10.8^0. These effects are easily explained by checking the acceptance of each programmed configuration and the behaviour is well reproduced by the XILINX prototype BTI simulation.

The average efficiency, in the fully covered geometrical range of Figure 5, that can be extracted from the data is given in Table 3: the efficiency in column 1 is the average efficiency in the full angular range, while the one in column 2 is restricted to the tracks with fitted angle in the full acceptance region for each configuration listed in Table 2.

θ(degrees)	Efficiency 1	Efficiency 2
0	91.5%	95.7%
10	80.1%	93.1%
20	79.3%	85.9%

Table 3 - Efficiency as a function of incident angle (see text for details).

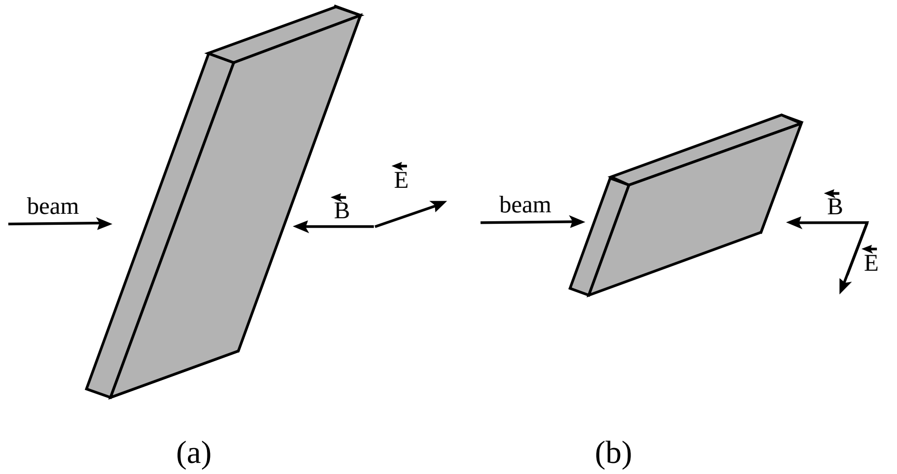

Figure 9 - Relative directions of beam, chamber, electric and magnetic fields in the test beam setup. Situation (a) corresponds to vertical wires and situation (b) corresponds to horizontal wires.

There is quite a large difference in the expected behaviour of the FPGA prototype and the designed full scale device. The latter is expected to have efficiencies similar or even better to the one quoted in the last column of Table 3, since there is no angular acceptance cut in its design.

4.5 Efficiency in Magnetic Field

Data were taken in magnetic field in the situations shown in Figure 9. The analysis of the prototype BTI performance was done on the data with the chamber at 20^0 with the beam. Unfortunately this configuration will be existing in CMS only in the longitudinal view, which is less important for the trigger, but it is the only one where good BTI data were available.

The effect of a magnetic field perpendicular to the wire direction is an elongation of the drift path of the electrons to the anode, resulting in a longer maximum drift time and therefore in an apparent modification of the drift velocity. These apparent changes and the efficiency are reported in Table 4. Instead the other magnetic field component introduces deviations from linearity of the space-time relationship.

The drift time deformation introduced at B = 0.5 T shifts T_{MAX} towards the nominal value programmed inside the BTI. Therefore the efficiency is expected to be higher than without field. In fact it is comparable between the two sets of data, while it clearly drops very fast for higher fields. Apparently the device is almost insensitive to fields as high as B=0.5 T even without changing its default programmation. Of course the drop in efficiency at higher fields can be recovered at least partially, as long as distorsions are limited, programming the BTI for the actual apparent drift velocity inside the field.

B(T)	T_{MAX}(ns)	V_d(μm/ns)	Efficiency 1	Efficiency 2
0.0	335	59.7	79.3%	85.9%
0.5	345	58.0	74.0%	80.7%
1.0	375	53.3	20.6%	11.4%
1.5	420	47.6	1.9%	0.1%

Table 4 - Apparent drift velocity modification and BTI efficiency as a function of magnetic field for $\theta = 20^0$ (see paragraph 4.4 for efficiency definition).

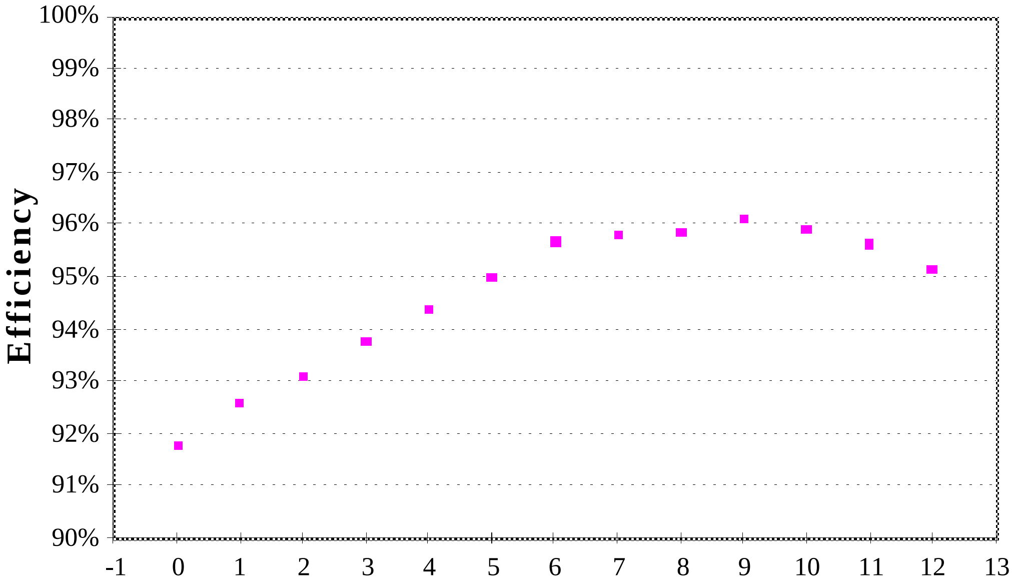

Figure 10- Full scale BTI simulation efficiency as a function of synchronization time.

5. Simulations of the Full Scale BTI

The data collected during the run were used as input to the simulation program of the full scale BTI. As in the case of the FPGA prototype the full scale device is supposed to have registers of programmable depth, set as a function of the drift velocity. In addition the device needs to be synchronized, and the current design of the CMS TTC device allows a fine setting of one nanosecond.

The BTI setup procedure was done in two steps using the data at B=0T: in the first one the depth of the shift register was determined, using the measured maximum drift time, and in the second one a fine setup was performed in order to define the synchronization .

The depth of the shift register can be set in steps of 12.5 ns and therefore the measured T_{MAX} is between step 26 and step 27 . We prepared a fixed sample of events that included an equal number of tracks for every available configuration at B=0T, to be as close as possible to a real situation. Then we compared the fraction of triggers at the expected step, using the two possible input parameters. The result of such an investigation leads to an efficiency of ~84% (using the parameter 26) and ~96% (using the parameter 27).

At this point, choosing the highest efficiency, the rates can be measured as a function of the synchronization time. The result of this fine tuning is shown in Figure 10 and looks quite similar to the one obtained for the FPGA device (see Figure 3).

The data provide information on the BTI behaviour in different magnetic field configurations. There are in fact three components of the field: one in the direction perpendicular to the chamber (B_n), one in the wire direction (B_w) and one in the direction perpendicular to the previous two components (B_z). In the case of vertical wires the magnetic field has the two components B_w=Bsinθ and B_n=Bcosθ, while in the case of horizontal wires the two components are B_z=Bsinθ and B_n=Bcosθ.

It is clear that a setup procedure could be performed in any of the situations considered in order to maximize the BTI efficiency. We have chosen to setup the device only once at B=0T in order to understand the extension of the range in which the BTI

	Inclination (degrees)				
	0	**10V**	**20V**	**10H**	**20H**
Magnetic field(T)					
0.0	92.7%			96.1%	95.8%
0.5	89.8%	87.2%	89.7%	94.9%	94.7%
1.0	69.7%	61.0%	67.1%	82.8%	78.4%
1.5			26.6%	29.9%	25.7%

Table 5 - Efficiency for bunch crossing identification in the simulation of the full scale BTI, using test data. The suffixes V(vertical) and H(horizontal) distinguish the situations that will occur in CMS for superlayers measuring in the transverse view(φ) and longitudinal view(θ) respectively.

performance was not significantly affected from drift lines deformations due the presence of a magnetic field. Furthermore this situation was the actual one in the test setup and this choice allows a direct comparison of the difference in performance between the FPGA prototype and the full scale device.

Having set up the device we then could run the simulation on all the available samples. The efficiency of the BTI is shown in Table 5.

Data were not available for B=1.5T and $\theta=0^0$ and $\theta=10^0$ with vertical wires, while we expect no difference for the inclined chamber with vertical wires at B=0T.

Looking at Table 5 we see that the BTI overall efficiency is sensitive to the magnetic field module rather than to the way its components are mixed.

In fact the efficiency is almost the same when the inclination introduces a magnetic field component in the wire direction. The apparent large gain in efficiency when the wire is in the horizontal position is explained by geometrical considerations.

When the wire is vertical, the chamber is normal to the beam and there is an inefficient zone caused by the cathode thickness. Indeed in this case two cathodes are hit in the chamber and therefore there are only two hits to be processed. This does not happen when the wire is horizontal and the chamber is inclined. The geometrically inefficient region accounts for about 5% of the covered area, thus explaining the apparent incoherence among the listed efficiencies.

A deeper analysis of the trigger output shows that the effect of the magnetic field is indeed more complicated. The output step is delayed from the elongation of the drift path, as shown in Figure 11, and therefore, while magnetic field increases, a larger contribution to triggers identifying correctly the bunch crossing is given by LTRGs. Furthermore different ratios af HTRGs and LTRGs are obtained for the various field configurations, pointing out that each field component acts in a different way.

Anyway the global effect of the magnetic field is small for fields up to 0.5 T, as expected from GARFIELD simulations of the cell. Therefore the device is expected to work without significant efficiency loss in an inhomogeneous field varying from 0T to 0.5 T, but the effect of the rest of the CMS muon trigger chain, and consequently on the global muon trigger efficiency, is not obvious.

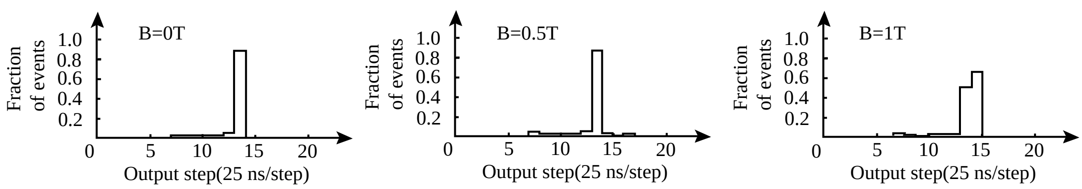

Figure 11 - Output step of HTRGs for different magnetic fields at $\theta=0^0$.

In addition the beam was unfortunately centred in a region of the chamber where there was one inefficient tube for all the data listed in Table 5. Only in the case of B=0T and $\theta=0^0$ we had data taken in a fully efficient chamber region. Running the simulation on this sample the BTI efficiency results to be 95.6%, consistent with the geometrical acceptance.

6. Conclusions

The beam test of the fixed angle prototype version of the BTI, realized in FPGA, was quite satisfactory, since its performance fully agrees with expectations. Once all the effects of the design limitations are considered, the efficiency of the device was very close to the geometrical efficiency.

The collected data were used to perform the simulation of the full scale device in a realistic environment. The result of the simulation confirms the validity of the design choices and is completely coherent with all the previously performed computations.